scientific reports

Check for updates

OPEN

Analysis of culture and RNA isolation methods for precision-cut liver slices from cirrhotic rats

Ben D. Leaker[1,2,6]✉, Yongtao Wang[3,4,6], Joshua Tam[2,5] & R. Rox Anderson[2,5]

Precision-cut liver slices (PCLS) are increasingly used as a model to investigate anti-fibrotic therapies. However, many studies use PCLS from healthy animals treated with pro-fibrotic stimuli in culture, which reflects only the early stages of fibrosis. The effects of different culture conditions on PCLS from cirrhotic animals has not been well characterized and there is no consensus on optimal methods. In this study, we report a method for the collection and culture of cirrhotic PCLS and compare the effect of common culture conditions on viability, function, and gene expression. Additionally, we compared three methods of RNA isolation and identified a protocol with high yield and purity. We observed significantly increased albumin production when cultured with insulin-transferrin-selenium and dexamethasone, and when incubated on a rocking platform. Culturing with insulin-transferrin-selenium and dexamethasone maintained gene expression closer to the levels in fresh slices. However, despite stable viability and function up to 4 days, we found significant changes in expression of key genes by day 2. Interestingly, we also observed that cirrhotic PCLS maintain viability in culture longer than slices from healthy animals. Due to the influence of matrix stiffness on fibrosis and hepatocellular function, it is important to evaluate prospective anti-fibrotic therapies in a platform that preserves tissue biomechanics. PCLS from cirrhotic animals represent a promising tool for the development of treatments for chronic liver disease.

Conventional cell culture systems lack the complexity of tissues, while preclinical animal models typically have limited throughput. In contrast, organ or tissue culture methods preserve complexity while allowing assays similar to those performed in cell cultures. Precision-cut liver slices (PCLS) is an ex vivo tissue culture model that is gaining popularity for the study of liver fibrosis. PCLS preserve the extracellular matrix and resident liver cell populations, providing a more accurate representation of the in vivo interactions between different cell types, and between cells and the matrix. PCLS also enable higher throughput and more easily controlled experiments than in vivo models as dozens of slices can be obtained from one animal. The primary drawbacks of PCLS are the limited time they can be cultured—typically a few days—as well as changes in expression that occur during culture.

PCLS have particularly attracted interest as a platform to test anti-fibrotic therapies. Many previous experiments have used healthy PCLS treated with pro-fibrotic stimuli, such as TGFβ and PDGF, to induce fibrosis ex vivo[1–9], or have relied on the spontaneous fibrosis activated in PCLS in culture[10–16]. Such experiments are useful to study the earliest onset of liver fibrosis but do not capture many of the effects of chronic liver disease in clinically relevant liver fibrosis. Chronic liver injury induces senescence of a variety of liver cell populations[17,18], and the long-term deposition of collagen and associated increase in tissue stiffness can suppress hepatocellular function through HNF4a and cytochrome P450[19–21]. There is also a critical positive feedback loop between fibrosis and matrix stiffness[22–25], which could significantly influence the effects of prospective anti-fibrotic therapies.

For a more clinically relevant model, PCLS can be collected from patient biopsies or from animal models after liver fibrosis or cirrhosis is induced in vivo. A variety of fibrosis etiologies have been investigated with this approach, including alcohol[26], hepatitis infection[27], non-alcoholic steatohepatitis (NASH)[26,28], cholestasis[29–33], and chemical hepatotoxins[26,34,35].

[1]Health Sciences and Technology, Harvard-Massachusetts Institute of Technology, Cambridge, MA, USA. [2]Wellman Center for Photomedicine, Massachusetts General Hospital, Thier Research Building, MGH, 55 Blossom Street, Boston, MA, USA. [3]Division of Gastrointestinal and Oncologic Surgery, Massachusetts General Hospital and Harvard Medical School, Boston, MA, USA. [4]Liver Center, Division of Gastroenterology, Massachusetts General Hospital and Harvard Medical School, Boston, MA, USA. [5]Department of Dermatology, Harvard Medical School, Boston, MA, USA. [6]These authors contributed equally: Ben D. Leaker and Yongtao Wang. ✉email: leakerb@mit.edu

The effects of different culture methods on PCLS from cirrhotic animals have not been well characterized. Prior work with fibrotic and cirrhotic slices often references the methods of experiments performed with slices from healthy animals, which may not be applicable given the significant differences between the healthy and cirrhotic liver in vivo. There is also no consensus on optimal culture conditions, most notably whether to include insulin and dexamethasone in the culture media. A direct comparison of the effect of culture conditions on viability, function, and gene expression of cirrhotic PCLS has not previously been performed.

To move towards standardized methodology, we report a method for the collection and culture of PCLS from cirrhotic rats. We compare the effect of culture media and rocking on PCLS viability and albumin production, as well as characterize changes in expression of key genes over time and when cultured with and without insulin-transferrin-selenium and dexamethasone. We also compare three methods for the isolation of RNA from cirrhotic PCLS and report a method capable of obtaining RNA with higher yield and purity than the standard RNeasy and TRIzol protocols.

Methods

Animals

This study is reported in accordance with applicable ARRIVE guidelines. All animal work was approved by the Massachusetts General Hospital Institutional Animal Care and Use Committee. All experiments were performed in accordance with relevant guidelines and regulations. For the cirrhotic experiments, 2 month old male Wistar rats were purchased from Charles River Laboratories. After a 1 week acclimatization period, cirrhosis was induced with biweekly intraperitoneal injections of thioacetamide at 200 mg/kg for 12 weeks followed by a 1 week wash out period. 4–5 month old male Wistar rats were used for healthy comparisons. Animals were housed in a controlled environment with food and water ad libitum. A total of 7 cirrhotic rats and 5 healthy rats were used for this study.

PCLS collection

Animals were euthanized via cardiac puncture under sterile conditions. The whole liver was harvested and 8 mm biopsy punches were used to obtain tissue columns. Columns were collected from the thickest portions of the medial and left lobe. The columns were immediately placed in chilled sterile Krebs Henseleit buffer (KHB; Sigma Aldrich, USA).

Columns were cut in half with a scalpel to obtain 2 shorter columns (Fig. 1a). These columns were mounted to the platform of a 7000smz-2 vibratome (Campden Instruments Limited, UK) with cyanoacrylate glue and the cutting tray of the vibratome was filled with chilled sterile KHB (Fig. 1b). The vibratome was fitted with a ceramic blade (Campden Instruments Limited) and run at 50 Hz frequency, 2.5 mm amplitude, 0.15 mm/s advance speed, 250 µm slice thickness (Fig. 1c). The first few slices were discarded to ensure a flat tissue surface. After cutting, slices were transferred to a sterile dish with chilled sterile KHB. A 6 mm biopsy punch was used to trim the final PCLS. This step ensures all PCLS are uniform in size, as the initial columns are often irregularly shaped (Fig. 1d). With such small samples, these irregular edges can result in significant differences in the total amount of tissue. This step also removes any tissue that may have come into contact with glue. The trimmed PCLS were then transferred to a 24 well plate with chilled sterile KHB until the end of collection. Approximately 20 uniform, viable slices were obtained per animal. One rat provides sufficient tissue to collect many more PCLS, but viability may be impacted by extended cutting times. For the isolation of human hepatocytes, Bhogal et al., 2011[36] reported a reduction in median cell viability from 53 to 25% for processing times greater than 3 h. Shorter times were not investigated. To ensure high quality slices, the total time from harvesting of the liver to the end of collecting PCLS was limited to approximately 1 h.

PCLS culture

PCLS were placed on an 8 µm-pore Transwell insert (Corning, USA) in a 12 well plate. All slices were cultured in 1 mL Williams' Medium E (Sigma Aldrich) with 2% FBS, 1% pen-strep, and 1% L-glutamine (Thermo Fisher, USA). Some slices were additionally cultured with 100 nM dexamethasone (Sigma Aldrich) and 1X insulin-transferrin-selenium-ethanolamine (Thermo Fisher)[35]. Plates were incubated under standard cell culture conditions either stationary or on a rocking platform. Media was changed every 24 h.

MTS viability assay

PCLS were placed in a 48 well plate with 400 µL culture media and 80 µL MTS reagent (Abcam, USA)[37]. The plates were incubated on a rocking platform under standard cell culture conditions for 1 h then the media was collected and absorbance was measured at 490 nm. Measurements were normalized to the viability of fresh slices.

Albumin ELISA

Media collected from the culture plate was centrifuged at 4 ℃, 400 g for 10 min. The supernatant was then stored at – 20 ℃ until ready to use. Albumin concentration was measured with a rat albumin ELISA kit (Abcam) according to manufacturer instructions.

Histology

PCLS were fixed in 4% formaldehyde overnight, embedded in paraffin, then cut to 10 µm sections. Sections were stained with hematoxylin & eosin (H&E) using standard methods.

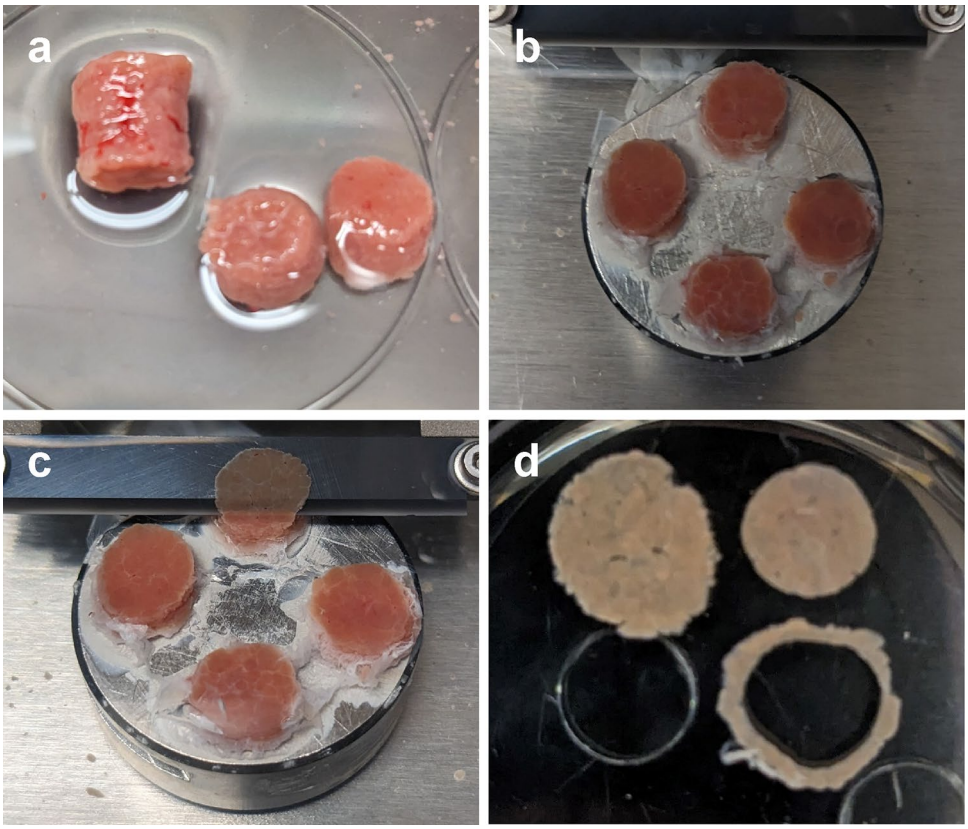

Figure 1. PCLS collection. (**a**) Tissue columns were harvested with an 8 mm biopsy punch then cut into 2 shorter columns. (**b**) Columns were mounted to the vibratome platform with cyanoacrylate glue. (**c**) 250 µm thick PCLS were cut at 50 Hz, 2.5 mm amplitude, 0.15 mm/s. (**d**) PCLS were trimmed with a 6 mm biopsy punch to ensure uniform slices.

RNA Isolation and qPCR

3 methods of RNA isolation were compared. The first method used the RNeasy micro kit (Qiagen, Germany) according to manufacturer instructions. The second method used TRIzol (Invitrogen, USA) according to the manufacturer instructions. The final method was a protocol reported by Ziros et al.[38] for the isolation of RNA from mouse thyroid, a very small organ which requires high yield RNA extraction. Briefly, PCLS were homogenized in TRIzol and frozen at −80 ℃ for at least 30 min. Phase separation was performed with 1-bromo-3-chloropropane (Sigma Aldrich) and the aqueous phase was purified using RNeasy micro spin columns. For all methods, PCLS were homogenized with TissueLyser II (Qiagen).

RNA concentration and purity were measured with NanoDrop (Thermo Fisher). RNA integrity was confirmed by gel electrophoresis on E-gel EX 2% agarose gels (Thermo Fisher).

cDNA was prepared from 1 µg total RNA using the SuperScript VILO IV kit (Thermo Fisher) according to manufacturer instructions. qPCR was then performed with TaqMan Fast Advanced Master Mix (Thermo Fisher) and TaqMan fluorescent probes for *Hnf4a* (Thermo Fisher; assay ID: Rn04339144_m1), *Cyp1a2* (Rn00561082_m1), *Lyve1* (Rn01510421_m1), *Tgfb1* (Rn00572010_m1), *Col1a1* (Rn01463848_m1), *Acta2* (Rn01759928_m1), *Cdkn1a* (Rn00589996_m1), and *Mki67* (Rn01451446_m1).

Stability analysis was performed with NormFinder[39] to determine appropriate reference genes. Fresh slices and PCLS after 4 days in culture were compared with TaqMan probes for *B2m* (Rn00560865_m1), *Ywhaz* (Rn00755072_m1), *Hprt1* (Rn01527840_m1), *Hmbs* (Rn01421873_g1), *18s* (Hs99999901_s1), *Sdha* (Rn00590475_m1), and *Ubc* (Rn01789812_g1). *Hprt1* and *Hmbs* were found to be the best combination of reference genes, with a stability value of 0.063.

Statistics

Student's t-test was performed to assess statistical significance with a p-value threshold of 0.05. The Benjamini–Hochberg procedure was used to correct for multiple comparisons in the qPCR experiments. Yield and purity metrics are expressed as mean ± standard deviation.

Results

Effect of culture conditions on cirrhotic PCLS viability and function

Two parameters were evaluated for their effect on cirrhotic PCLS viability and function: media supplements (insulin-transferrin-selenium-ethanolamine and dexamethasone) and incubation on a rocking platform. PCLS cultured with these supplements had no significant difference in overall viability after 4 days in culture (Fig. 2a) but the supplemented media significantly increased PCLS function at all timepoints (Fig. 2b). Similarly,

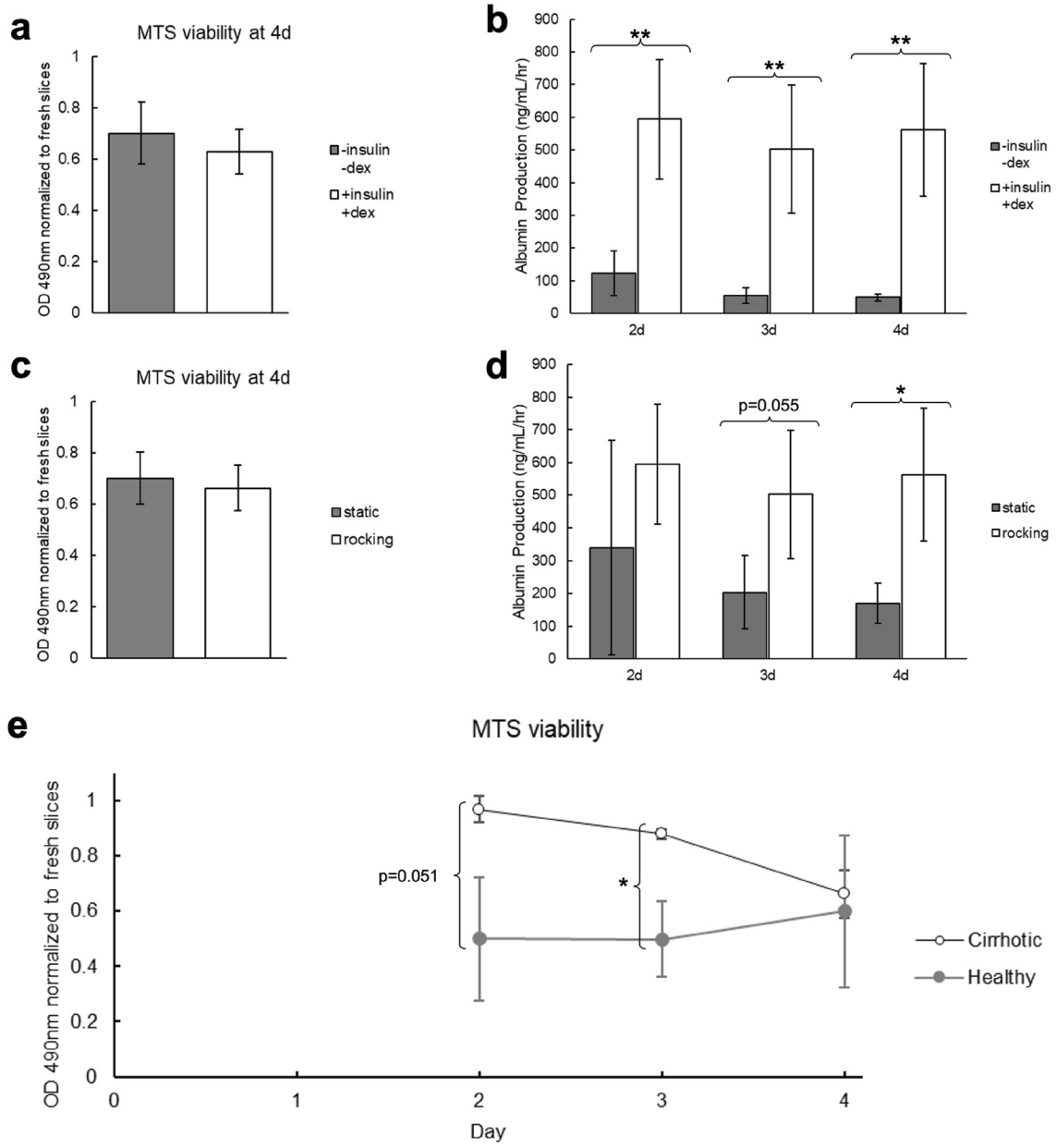

Figure 2. Comparison of culture conditions for cirrhotic PCLS viability and function. (**a,b**) Cirrhotic PCLS viability and function when cultured with and without insulin-transferrin-selenium-ethanolamine and dexamethasone. Both groups were incubated on a rocking platform. (**a**) Viability measured by MTS assay after 4 days in culture normalized to the viability of fresh PCLS. There is no significant difference in slice viability. (**b**) ELISA for albumin secreted into the media over 4 days in culture. Culturing with insulin-transferrin-selenium-ethanolamine and dexamethasone significantly increases PCLS function at all timepoints. (**c,d**) Cirrhotic PCLS viability and function when incubated on a rocking platform or static. Both groups were cultured with insulin-transferrin-selenium-ethanolamine and dexamethasone. (**c**) Viability measured by MTS assay after 4 days in culture. There is no significant difference in slice viability. (**d**) ELISA for albumin secreted into the media over 4 days in culture. Culturing on a rocking platform significantly increased PCLS function at the 4 day timepoint. (**e**) Viability of healthy and cirrhotic PCLS measured by MTS assay over 4 days in culture normalized to viability of fresh healthy and cirrhotic PCLS, respectively. The cirrhotic slices maintain higher viability until day 4. $^{*}p < 0.05$, $^{**}p < 0.01$.

incubation on a rocking platform did not have an effect on the overall viability (Fig. 2c) but preserved PCLS function at later timepoints (Fig. 2d).

Interestingly, we also found that cirrhotic PCLS maintained higher viability in culture than PCLS from healthy animals until day 4 (Fig. 2e). This may be related to the poor perfusion and hypoxic environment of the cirrhotic liver in vivo[40–43]. Survival in culture is heavily dependent on oxygen delivery to the tissue, so it is possible that adaptation to hypoxia in vivo enables better survival ex vivo.

H&E images are provided in Supplementary Fig. 1. Between 2d and 4d, some small areas of necrosis develop in the PCLS cultured with supplemented media on a rocking platform. Much larger regions of necrosis are evident in the unsupplemented PCLS and static cultured PCLS. The structural integrity of these slices was also significantly deteriorated compared to the supplemented and rocking PCLS.

Comparison of RNA isolation methods for cirrhotic PCLS

RNA yield and purity for three isolation methods—Qiagen RNeasy kit, standard TRIzol protocol, and the small tissue RNA isolation protocol described by Ziros et al. for the isolation of high-quality RNA from mouse thyroid—were compared with cirrhotic PCLS after 4 days in culture (Table 1). The RNeasy protocol produced high purity RNA, but with very low yield. Conversely, the TRIzol protocol gave higher yield but with poor purity. The protocol described by Ziros et al. gave the highest yield and purity of all 3 protocols. To determine whether the difference in purity would significantly alter expression measurements, RNA isolated by the TRIzol and Ziros et al. protocols were compared with qPCR. Of the 8 genes measured, 1 was found to have a statistically significant difference in expression after multiple hypothesis correction (Supplementary Fig. 2). We also found that there is a significant decrease in RNA yield from PCLS in culture compared to fresh slices in addition to a small but statistically significant decrease in A260/280 (Supplementary Table 1).

These methods were also compared for healthy slices, and we again found that the Ziros et al. protocol gave the best combination of yield and RNA purity for both 1d and 4d in culture (Supplementary Table 2, 3).

Effect of culture media on expression in cirrhotic PCLS

Expression of 8 key genes related to liver function and fibrosis were evaluated by qPCR for cirrhotic slices cultured for 4 days with and without insulin-transferrin-selenium-ethanolamine and dexamethasone (Fig. 3). In all cases with statistically significant differences, culturing with these supplements resulted in expression more similar to fresh slices. *Hnf4a* and *Cyp1a2*, markers of hepatocyte function and differentiation, were increased with the supplemented media. *Tgfb1*, a key gene associated with the spontaneous ex vivo fibrosis response, was reduced with the supplemented media, as well as *Mki67*, a marker of proliferation. There were no statistically significant differences in expression of *Lyve1*, a marker of liver sinusoidal endothelium, *Col1a1* and *Acta2*, markers of fibrosis, or *Cdkn1a* (p21), a marker of senescence.

Time course of expression changes in cirrhotic PCLS

Expression of these 8 genes were measured at the 2 and 4 day timepoints to characterize how expression changes over time in culture (Fig. 4). For these results, all slices were cultured with insulin-transferrin-selenium-ethanolamine and dexamethasone, and were incubated on a rocking platform. We found that despite stable viability and function, there are already significant differences in many genes by the 2 day timepoint. *Hnf4a* and *Cyp1a2* are significantly downregulated compared to fresh slices by day 2, and expression further decreases by day 4. *Lyve1* expression is only significantly decreased at the 4 day timepoint. Significantly elevated expression of *Tgfb1*, *Col1a1*, and *Acta2* is not observed until the 4 day timepoint, indicating that the ex vivo spontaneous pro-fibrotic stimuli induce a relatively slow process in cirrhotic PCLS. *Cdkn1a* expression is significantly elevated by day 2 and there is no significant difference in expression between the 2 and 4 day timepoints. Interestingly, *Mki67* expression is decreased at the 2 day timepoint but increased by day 4.

Discussion

The PCLS model has been discussed in literature for many years. Dewyse et al., 2021[44] provides an extensive review of prior work establishing appropriate culture methods. However, the bulk of this work has been performed with healthy tissue. Due to the lack of comparison of culture methods for fibrotic and cirrhotic PCLS, many publications using these tissue types rely on the methods reported for healthy tissue, such as the protocol described by de Graaf et al., 2010[45]. Given the significant differences between healthy and cirrhotic liver in vivo, appropriate culture methods need to be validated with cirrhotic PCLS.

RNA isolation protocol	Yield (µg/mg tissue)	A260/280	A260/230
Qiagen RNeasy	0.2 ± 0.1	2.01 ± 0.03	1.7 ± 0.4
TRIzol	1.5 ± 0.1	1.89 ± 0.03	0.6 ± 0.1
Ziros et al	2.3 ± 0.9*	2.03 ± 0.03†	1.9 ± 0.4†

Table 1. Yield and purity metrics for three methods of RNA isolation from cirrhotic PCLS after 4 days in culture. The protocol described by Ziros et al. gives the highest yield and RNA purity. *$p < 0.05$ comparing Ziros et al. and Qiagen RNeasy protocols, †$p < 0.05$ comparing Ziros et al. and Trizol.

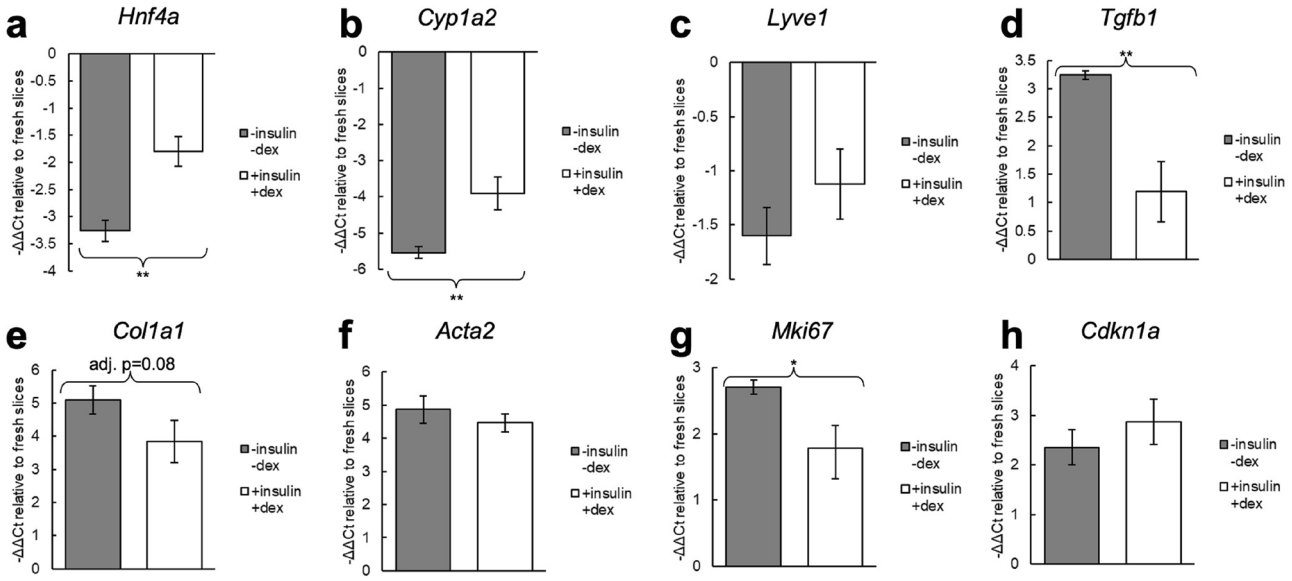

Figure 3. Expression changes in cirrhotic PCLS after 4 days in culture with and without insulin-transferrin-selenium-ethanolamine and dexamethasone. Both groups were incubated on a rocking platform. ΔΔCt values were calculated relative to fresh slices. For all genes with statistically significant differences, culturing with insulin-transferrin-selenium-ethanolamine and dexamethasone maintained expression closer to fresh slices. Statistical tests were performed on the ΔCt values. *$p < 0.05$, **$p < 0.01$.

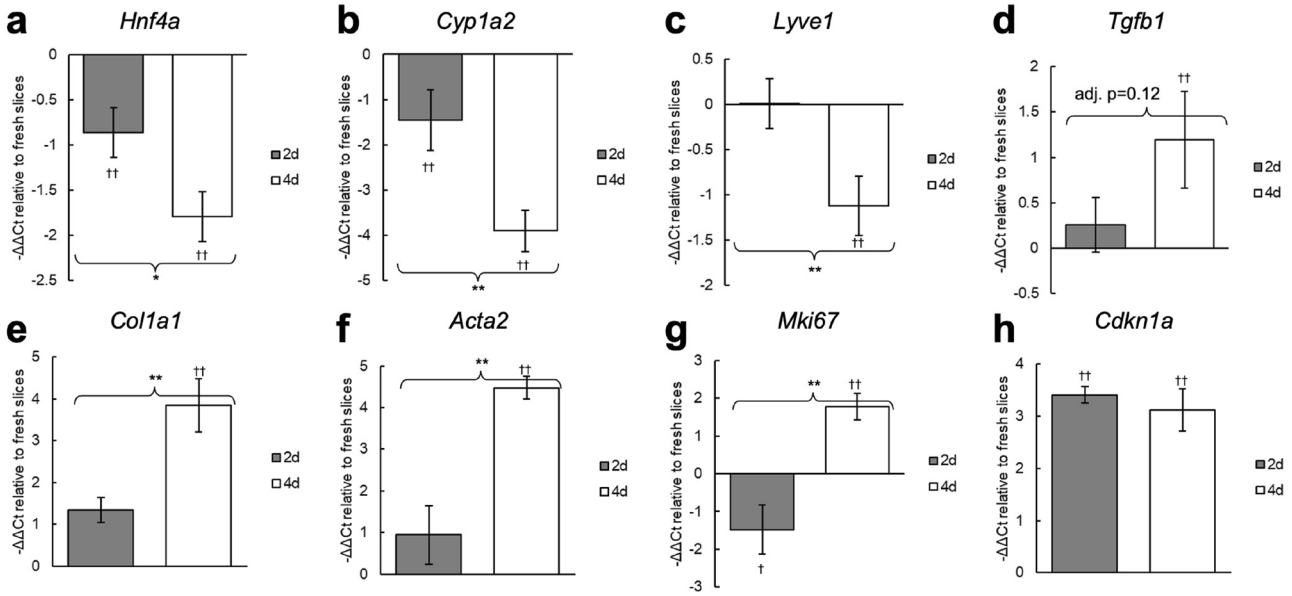

Figure 4. Expression changes in cirrhotic PCLS at 2 and 4 days in culture. Slices were cultured with insulin-transferrin-selenium-ethanolamine and dexamethasone, and were incubated on a rocking platform. ΔΔCt values were calculated relative to fresh slices. Statistical tests were performed on the ΔCt values. *$p < 0.05$, **$p < 0.01$; $^{\dagger}p < 0.05$ compared to fresh slices, $^{\dagger\dagger}p < 0.01$ compared to fresh slices.

In this work we characterized the performance of cirrhotic PCLS in culture and clarified the effect of different commonly used culture conditions. We describe a method for the collection and culture of cirrhotic PCLS that are viable with stable function for up to 4 days. Our results show that there is a clear benefit to culturing with insulin-transferrin-selenium and dexamethasone as well as incubating on a rocking platform. This method significantly improved albumin production and maintained expression of *Hnf4a*, *Cyp1a2*, *Tgfb1*, and *Mki67* closer to the level in fresh slices. Insulin promotes nutrient uptake, while transferrin and selenium inhibit toxic reactive oxygen species formation[46,47]. Insulin-transferrin-selenium supplemented media has been used in some PCLS literature over the last few decades, but many more published studies do not include these supplements. De Graaf et al., 2010[45] recommended supplementing media for experiments requiring more than 48 h in culture. We have found that, at least for cirrhotic PCLS, there is already a significant difference in PCLS performance with

and without these supplements at this timepoint. Our results suggest these methods would be beneficial unless they are contraindicated by the specific hypothesis under investigation (e.g., insulin interfering with a signaling pathway of interest). The importance of shaking or rocking has long been established and is consistently used in published literature for both healthy and fibrotic PCLS.

Tissue oxygenation is a critical factor in maintaining viability of PCLS. To address this, the majority of prior work incubated PCLS under 80–95% oxygen. As an alternative protocol, Wu et al., 2018[48] cultured PCLS on permeable inserts so that the tissue sits near the media-air interface. While not the first to use inserts, prior work had submerged slices in media rather than placing them near the interface. They found that this resulted in long-term viability under standard cell culture conditions. This approach has since been employed in several other studies[9,27,49]. Enabling the use of standard culture conditions improves the practicality of the PCLS model given the ubiquity of cell culture incubators. In addition, it has been speculated that culturing PCLS at oxygen concentrations far above physiological levels may influence experimental results, but the benefits to viability have warranted its use[50]. Mathematical modelling suggests the insert approach results in a more physiologically accurate oxygen concentration within the PCLS[51]. The effects on tissue function and expression of high concentrations of oxygen compared to the insert method should be investigated in future experiments.

Viability and albumin production are the most commonly used methods in prior work to characterize the performance of PCLS in culture. However, we also investigated changes in expression of key liver genes and found several important changes that are not reflected by these assays. Despite high albumin production throughout the time in culture, there was progressive decline in expression of *Hnf4a* and *Cyp1a2*, two key regulators of hepatocellular function. This is possibly due to the same process of dedifferentiation that is commonly observed with primary hepatocytes in culture[52–56]. We also found that the senescence marker *Cdkn1a* is upregulated at both day 2 and 4. Hepatocyte senescence is associated with a pro-inflammatory secretory state, declining function, and suppressed proliferation[18,57]. Interestingly, we observed that the proliferation marker *Mki67* is downregulated at the 2 day timepoint, but becomes upregulated by day 4. This biphasic response may indicate differing proliferative states for different cell populations. It is possible that hepatocyte senescence drives *Mki67* expression down at day 2, while a delayed fibrotic response—demonstrated by upregulation of *Tgfb1*, *Col1a1*, and *Acta2*—activates proliferation of stellate cells at the 4 day timepoint. We also found that *Lyve1* is downregulated at day 4. *Lyve1* is a marker of liver sinusoidal endothelial cells, and its downregulation is associated with capillarization of sinusoids[58,59]. This may indicate some damage or dedifferentiation is occurring to the sinusoidal endothelium in culture.

These results demonstrate that different metrics provide different results for the stability of PCLS in culture. Viability and albumin production remain high up to 4 days in culture. However, when compared to fresh slices there are significant changes in expression of key genes as early as day 2. It is difficult to reconcile these data to produce a single number for the time cirrhotic PCLS can be cultured. An appropriate timeline needs to be determined on a case-by-case basis depending on the specific hypothesis and metrics under investigation.

We have also reported a protocol for RNA isolation with higher yield and purity than the standard RNeasy and TRIzol protocols. High yield is necessary to extract sufficient RNA for quality control and downstream assays from small tissue samples, while high purity is required to prevent contaminants from interfering in expression measurements. The general guideline for pure RNA is $A^{260}/_{280}$ around 2.0 and $A^{260}/_{230}$ between 1.8 and 2.2[60]. With the protocol described by Ziros et al., we were able to obtain RNA with $A^{260}/_{280}$ of 2.03 ± 0.03 and $A^{260}/_{230}$ of 1.9 ± 0.4 (Table 1) after 4d in culture. It should be noted that these ratios depend on the concentration of both RNA and contaminants—so trace amounts of a contaminant could significantly skew the purity ratio if the RNA concentration is also low. Consequently, using larger PCLS samples (e.g., 8 mm diameter instead of the 6 mm diameter used here) may give higher purity ratios in addition to increasing total RNA yield. Typical contaminants that absorb at 230 nm are phenol and guanidine thiocyanate found in lysis buffers. In high quantities these contaminants can inhibit PCR and give misleading expression results.

We also showed that cirrhotic slices maintain viability in culture longer than slices from healthy animals. This may be due to adaptation in vivo to the hypoxic and poorly perfused cirrhotic liver[40–43]. This enhanced survival ex vivo adds to the benefits of PCLS from cirrhotic or fibrotic animals as a more appropriate model to test antifibrotic therapies than PCLS from healthy animals. Though some previous studies have used healthy PCLS to test antifibrotic therapies, this approach likely has limited application to clinically relevant liver fibrosis. The collagen deposition and increasing tissue stiffness in chronic liver fibrosis have a variety of effects on the liver. There is a crucial positive feedback loop between matrix stiffness and collagen deposition—increasing stiffness causes pro-fibrotic signaling, leading to collagen deposition and further increasing stiffness[22–25]—which would not be established in PCLS from healthy animals. For this reason, treatments that can suppress fibrosis in soft tissues may be less effective in stiff tissues. Matrix stiffness also influences hepatocyte phenotype, with a stiffer matrix leading to loss of hepatocyte-specific functions[19–21]. This would be important for functional outcome metrics and toxicology. These aspects are unlikely to sufficiently develop in healthy slices over just a few days in culture but can be captured with fibrosis induced in vivo.

PCLS are a promising platform for the future of antifibrotic therapy development. The interactions between different cell populations as well as interactions with their microenvironment is a crucial part of the response to disease, injury, and treatment. Especially in the setting of fibrosis, cell–matrix biomechanics plays an important regulatory role. Other methods that attempt to address this include organoids and 3D co-culture platforms that mimic parts of the in vivo liver[61–63]. PCLS is a relatively simple technique that directly captures all liver cell populations in their native architecture. PCLS also has the benefit of being able to be used with human liver biopsies—enabling new compounds to be tested on human tissue and potentially opening the possibility of personalized medicine applications.

Cirrhotic PCLS also offer several advantages over in vivo models. Cirrhosis takes several months to develop in mice and rats. With the PCLS model, each cirrhotic animal can provide dozens of PCLS which can be divided

between many different experimental groups. This enables higher throughput testing of new drugs, while also reducing the number of required animals. Where appropriate, PCLS also provide the opportunity for highly controlled experiments as nearly identical serial slices can be tested under multiple conditions. Ultimately PCLS are not a replacement for in vivo testing—given the lack of circulating immune cells and inability to identify potential toxicity outside the liver, among other drawbacks—but they enable faster and easier screening of compounds in a realistic and meaningful ex vivo platform which can substantially reduce the number of animals required for drug development.

Data availability

The datasets generated during and/or analyzed during the current study are available from the corresponding author on reasonable request.

Received: 11 September 2023; Accepted: 28 June 2024
Published online: 03 July 2024

References

1. Sadasivan, S. K. *et al.* Developing an in vitro screening assay platform for evaluation of antifibrotic drugs using precision-cut liver slices. *Fibrogenesis Tissue Repair* **8**, 1. https://doi.org/10.1186/s13069-014-0017-2 (2015).
2. van de Bovenkamp, M., Groothuis, G. M., Meijer, D. K. & Olinga, P. Liver slices as a model to study fibrogenesis and test the effects of anti-fibrotic drugs on fibrogenic cells in human liver. *Toxicol. Vitr.* **22**, 771–778. https://doi.org/10.1016/j.tiv.2007.11.019 (2008).
3. Guo, Y. *et al.* Protective effect of sodium ferulate on acetaldehyde-treated precision-cut rat liver slices. *J. Med. Food* **15**, 557–562. https://doi.org/10.1089/jmf.2011.1915 (2012).
4. Westra, I. M., Oosterhuis, D., Groothuis, G. M. & Olinga, P. Precision-cut liver slices as a model for the early onset of liver fibrosis to test antifibrotic drugs. *Toxicol. Appl. Pharmacol.* **274**, 328–338. https://doi.org/10.1016/j.taap.2013.11.017 (2014).
5. Coombes, J. D. *et al.* Osteopontin is a proximal effector of leptin-mediated non-alcoholic steatohepatitis (NASH) fibrosis. *Biochim. Biophys. Acta* **1862**, 135–144. https://doi.org/10.1016/j.bbadis.2015.10.028 (2016).
6. De Chiara, F. *et al.* Ammonia scavenging prevents progression of fibrosis in experimental nonalcoholic fatty liver disease. *Hepatology* **71**, 874–892. https://doi.org/10.1002/hep.30890 (2020).
7. Wang, K., Lin, B., Brems, J. J. & Gamelli, R. L. Hepatic apoptosis can modulate liver fibrosis through TIMP1 pathway. *Apoptosis* **18**, 566–577. https://doi.org/10.1007/s10495-013-0827-5 (2013).
8. Luangmonkong, T. *et al.* In vitro and ex vivo anti-fibrotic effects of LY2109761, a small molecule inhibitor against TGF-β. *Toxicol. Appl. Pharmacol.* **355**, 127–137. https://doi.org/10.1016/j.taap.2018.07.001 (2018).
9. Barcena-Varela, M. *et al.* Epigenetic mechanisms and metabolic reprogramming in fibrogenesis: Dual targeting of G9a and DNMT1 for the inhibition of liver fibrosis. *Gut* **70**, 388–400. https://doi.org/10.1136/gutjnl-2019-320205 (2021).
10. Gore, E. *et al.* PI3K inhibition reduces murine and human liver fibrogenesis in precision-cut liver slices. *Biochem. Pharmacol.* **169**, 113633. https://doi.org/10.1016/j.bcp.2019.113633 (2019).
11. Starokozhko, V. *et al.* Viability, function and morphological integrity of precision-cut liver slices during prolonged incubation: Effects of culture medium. *Toxicol. Vitr.* **30**, 288–299. https://doi.org/10.1016/j.tiv.2015.10.008 (2015).
12. Bigaeva, E. *et al.* Transcriptomic characterization of culture-associated changes in murine and human precision-cut tissue slices. *Arch. Toxicol.* **93**, 3549–3583. https://doi.org/10.1007/s00204-019-02611-6 (2019).
13. Westra, I. M. *et al.* Human precision-cut liver slices as a model to test antifibrotic drugs in the early onset of liver fibrosis. *Toxicol. Vitr.* **35**, 77–85. https://doi.org/10.1016/j.tiv.2016.05.012 (2016).
14. Bigaeva, E. *et al.* Exploring organ-specific features of fibrogenesis using murine precision-cut tissue slices. *Biochim. Biophys. Acta Mol. Basis Dis.* **1866**, 165582. https://doi.org/10.1016/j.bbadis.2019.165582 (2020).
15. Stefanovic, B., Manojlovic, Z., Vied, C., Badger, C. D. & Stefanovic, L. Discovery and evaluation of inhibitor of LARP6 as specific antifibrotic compound. *Sci. Rep.* **9**, 326. https://doi.org/10.1038/s41598-018-36841-y (2019).
16. Vilaseca, M. *et al.* Mitochondria-targeted antioxidant mitoquinone deactivates human and rat hepatic stellate cells and reduces portal hypertension in cirrhotic rats. *Liver Int.* **37**, 1002–1012. https://doi.org/10.1111/liv.13436 (2017).
17. Aravinthan, A. D. & Alexander, G. J. M. Senescence in chronic liver disease: Is the future in aging?. *J. Hepatol.* **65**, 825–834. https://doi.org/10.1016/j.jhep.2016.05.030 (2016).
18. Huda, N. *et al.* Hepatic senescence, the good and the bad. *World J. Gastroenterol.* **25**, 5069–5081. https://doi.org/10.3748/wjg.v25.i34.5069 (2019).
19. Desai, S. S. *et al.* Physiological ranges of matrix rigidity modulate primary mouse hepatocyte function in part through hepatocyte nuclear factor 4 alpha. *Hepatology* **64**, 261–275. https://doi.org/10.1002/hep.28450 (2016).
20. Semler, E. J., Lancin, P. A., Dasgupta, A. & Moghe, P. V. Engineering hepatocellular morphogenesis and function via ligand-presenting hydrogels with graded mechanical compliance. *Biotechnol. Bioeng.* **89**, 296–307. https://doi.org/10.1002/bit.20328 (2005).
21. Semler, E. J., Ranucci, C. S. & Moghe, P. V. Mechanochemical manipulation of hepatocyte aggregation can selectively induce or repress liver-specific function. *Biotechnol. Bioeng.* **69**, 359–369. https://doi.org/10.1002/1097-0290(20000820)69:4%3c359::aid-bit2%3e3.0.co;2-q (2000).
22. Liu, F. *et al.* Feedback amplification of fibrosis through matrix stiffening and COX-2 suppression. *J. Cell Biol.* **190**, 693–706 (2010).
23. Hinz, B. & Gabbiani, G. Mechanisms of force generation and transmission by myofibroblasts. *Curr. Opin. Biotechnol.* **14**, 538–546. https://doi.org/10.1016/j.copbio.2003.08.006 (2003).
24. Li, Z. *et al.* Transforming growth factor-beta and substrate stiffness regulate portal fibroblast activation in culture. *Hepatology* **46**, 1246–1256. https://doi.org/10.1002/hep.21792 (2007).
25. Arora, P. D., Narani, N. & McCulloch, C. A. The compliance of collagen gels regulates transforming growth factor-beta induction of alpha-smooth muscle actin in fibroblasts. *Am. J. Pathol.* **154**, 871–882. https://doi.org/10.1016/s0002-9440(10)65334-5 (1999).
26. Guo, Y., Wang, H. & Zhang, C. Establishment of rat precision-cut fibrotic liver slice technique and its application in verapamil metabolism. *Clin. Exp Pharmacol. Physiol.* **34**, 406–413. https://doi.org/10.1111/j.1440-1681.2007.04582.x (2007).
27. Wu, X. *et al.* Response of human liver tissue to innate immune stimuli. *Front. Immunol.* **13**, 811551. https://doi.org/10.3389/fimmu.2022.811551 (2022).
28. Gore, E. *et al.* Investigating fibrosis and inflammation in an ex vivo NASH murine model. *Am. J. Physiol. Gastrointest. Liver Physiol.* **318**, G336-g351. https://doi.org/10.1152/ajpgi.00209.2019 (2020).
29. Westra, I. M., Oosterhuis, D., Groothuis, G. M. & Olinga, P. The effect of antifibrotic drugs in rat precision-cut fibrotic liver slices. *PLoS ONE* **9**, e95462. https://doi.org/10.1371/journal.pone.0095462 (2014).
30. van de Bovenkamp, M., Groothuis, G. M., Meijer, D. K. & Olinga, P. Precision-cut fibrotic rat liver slices as a new model to test the effects of anti-fibrotic drugs in vitro. *J. Hepatol.* **45**, 696–703. https://doi.org/10.1016/j.jhep.2006.04.009 (2006).

31. Huang, X. *et al.* Molecular characterization of a precision-cut rat liver slice model for the evaluation of antifibrotic compounds. *Am. J. Physiol. Gastrointest. Liver Physiol.* **316**, G15-g24. https://doi.org/10.1152/ajpgi.00281.2018 (2019).
32. Hagens, W. I. *et al.* Gliotoxin non-selectively induces apoptosis in fibrotic and normal livers. *Liver Int.* **26**, 232–239. https://doi.org/10.1111/j.1478-3231.2005.01212.x (2006).
33. Gonzalo, T. *et al.* Local inhibition of liver fibrosis by specific delivery of a platelet-derived growth factor kinase inhibitor to hepatic stellate cells. *J. Pharmacol. Exp. Ther.* **321**, 856–865. https://doi.org/10.1124/jpet.106.114496 (2007).
34. Oldenburger, A. *et al.* Modulation of vascular contraction via soluble guanylate cyclase signaling in a novel ex vivo method using rat precision-cut liver slices. *Pharmacol. Res. Perspect.* **9**, e00768. https://doi.org/10.1002/prp2.768 (2021).
35. Paish, H. L. *et al.* A bioreactor technology for modeling fibrosis in human and rodent precision-cut liver slices. *Hepatology* **70**, 1377–1391. https://doi.org/10.1002/hep.30651 (2019).
36. Bhogal, R. H. *et al.* Isolation of primary human hepatocytes from normal and diseased liver tissue: A one hundred liver experience. *PLoS ONE* **6**, e18222. https://doi.org/10.1371/journal.pone.0018222 (2011).
37. Kenerson, H. L., Sullivan, K. M., Labadie, K. P., Pillarisetty, V. G. & Yeung, R. S. Protocol for tissue slice cultures from human solid tumors to study therapeutic response. *STAR Protoc.* **2**, 100574. https://doi.org/10.1016/j.xpro.2021.100574 (2021).
38. Ziros, P. G., Chartoumpekis, D. V. & Sykiotis, G. P. A simple protocol for high efficiency protein isolation after RNA isolation from mouse thyroid and other very small tissue samples. *Methods Mol. Biol.* **1449**, 383–393. https://doi.org/10.1007/978-1-4939-3756-1_25 (2016).
39. Andersen, C. L., Jensen, J. L. & Ørntoft, T. F. Normalization of real-time quantitative reverse transcription-PCR data: A model-based variance estimation approach to identify genes suited for normalization, applied to bladder and colon cancer data sets. *Cancer Res.* **64**, 5245–5250. https://doi.org/10.1158/0008-5472.Can-04-0496 (2004).
40. Sherman, I. A., Pappas, S. C. & Fisher, M. M. Hepatic microvascular changes associated with development of liver fibrosis and cirrhosis. *Am. J. Physiol.* **258**, H460-465. https://doi.org/10.1152/ajpheart.1990.258.2.H460 (1990).
41. Vollmar, B., Siegmund, S. & Menger, M. D. An intravital fluorescence microscopic study of hepatic microvascular and cellular derangements in developing cirrhosis in rats. *Hepatology* **27**, 1544–1553. https://doi.org/10.1002/hep.510270612 (1998).
42. Iwakiri, Y. & Groszmann, R. J. Vascular endothelial dysfunction in cirrhosis. *J. Hepatol.* **46**, 927–934. https://doi.org/10.1016/j.jhep.2007.02.006 (2007).
43. Cai, J., Hu, M., Chen, Z. & Ling, Z. The roles and mechanisms of hypoxia in liver fibrosis. *J. Transl. Med.* **19**, 186. https://doi.org/10.1186/s12967-021-02854-x (2021).
44. Dewyse, L. *et al.* Improved precision-cut liver slice cultures for testing drug-induced liver fibrosis. *Front. Med. (Lausanne)* **9**, 862185. https://doi.org/10.3389/fmed.2022.862185 (2022).
45. de Graaf, I. A. *et al.* Preparation and incubation of precision-cut liver and intestinal slices for application in drug metabolism and toxicity studies. *Nat. Protoc.* **5**, 1540–1551. https://doi.org/10.1038/nprot.2010.111 (2010).
46. Aisen, P., Enns, C. & Wessling-Resnick, M. Chemistry and biology of eukaryotic iron metabolism. *Int. J. Biochem. Cell Biol.* **33**, 940–959. https://doi.org/10.1016/s1357-2725(01)00063-2 (2001).
47. Baker, R. D. Jr., Baker, S. S. & Rao, R. Selenium deficiency in tissue culture: Implications for oxidative metabolism. *J. Pediatr. Gastroenterol. Nutr.* **27**, 387–392. https://doi.org/10.1097/00005176-199810000-00003 (1998).
48. Wu, X. *et al.* Precision-cut human liver slice cultures as an immunological platform. *J. Immunol. Methods* **455**, 71–79. https://doi.org/10.1016/j.jim.2018.01.012 (2018).
49. Wang, G. *et al.* Tumour extracellular vesicles and particles induce liver metabolic dysfunction. *Nature* **618**, 374–382. https://doi.org/10.1038/s41586-023-06114-4 (2023).
50. Szalowska, E. *et al.* Effect of oxygen concentration and selected protocol factors on viability and gene expression of mouse liver slices. *Toxicol. Vitr.* **27**, 1513–1524. https://doi.org/10.1016/j.tiv.2013.03.007 (2013).
51. Chidlow, S. J., Randle, L. E. & Kelly, R. A. Predicting physiologically-relevant oxygen concentrations in precision-cut liver slices using mathematical modelling. *PLoS ONE* **17**, e0275788. https://doi.org/10.1371/journal.pone.0275788 (2022).
52. Elaut, G. *et al.* Molecular mechanisms underlying the dedifferentiation process of isolated hepatocytes and their cultures. *Curr. Drug Metab.* **7**, 629–660. https://doi.org/10.2174/138920006778017759 (2006).
53. Heslop, J. A. *et al.* Mechanistic evaluation of primary human hepatocyte culture using global proteomic analysis reveals a selective dedifferentiation profile. *Arch. Toxicol.* **91**, 439–452. https://doi.org/10.1007/s00204-016-1694-y (2017).
54. Kiamehr, M. *et al.* Dedifferentiation of primary hepatocytes is accompanied with reorganization of lipid metabolism indicated by altered molecular lipid and miRNA profiles. *Int. J. Mol. Sci.* https://doi.org/10.3390/ijms20122910 (2019).
55. Irvine, K. M. *et al.* Senescent human hepatocytes express a unique secretory phenotype and promote macrophage migration. *World J. Gastroenterol.* **20**, 17851–17862. https://doi.org/10.3748/wjg.v20.i47.17851 (2014).
56. Cieslak, K. P., Baur, O., Verheij, J., Bennink, R. J. & van Gulik, T. M. Liver function declines with increased age. *HPB (Oxford)* **18**, 691–696. https://doi.org/10.1016/j.hpb.2016.05.011 (2016).
57. Bonnet, L. *et al.* Cellular senescence in hepatocytes contributes to metabolic disturbances in NASH. *Front. Endocrinol. (Lausanne)* **13**, 957616. https://doi.org/10.3389/fendo.2022.957616 (2022).
58. Mouta Carreira, C. *et al.* LYVE-1 is not restricted to the lymph vessels: Expression in normal liver blood sinusoids and down-regulation in human liver cancer and cirrhosis. *Cancer Res.* **61**, 8079–8084 (2001).
59. Arimoto, J. *et al.* Expression of LYVE-1 in sinusoidal endothelium is reduced in chronically inflamed human livers. *J. Gastroenterol.* **45**, 317–325. https://doi.org/10.1007/s00535-009-0152-5 (2010).
60. Unger, C., Lokmer, N., Lehmann, D. & Axmann, I. M. Detection of phenol contamination in RNA samples and its impact on qRT-PCR results. *Anal. Biochem.* **571**, 49–52. https://doi.org/10.1016/j.ab.2019.02.002 (2019).
61. Bao, Y. L. *et al.* Animal and organoid models of liver fibrosis. *Front. Physiol.* **12**, 666138. https://doi.org/10.3389/fphys.2021.666138 (2021).
62. Ma, Y. *et al.* Three-dimensional cell co-culture liver models and their applications in pharmaceutical research. *Int. J. Mol. Sci.* https://doi.org/10.3390/ijms24076248 (2023).
63. Godoy, P. *et al.* Recent advances in 2D and 3D in vitro systems using primary hepatocytes, alternative hepatocyte sources and non-parenchymal liver cells and their use in investigating mechanisms of hepatotoxicity, cell signaling and ADME. *Arch. Toxicol.* **87**, 1315–1530. https://doi.org/10.1007/s00204-013-1078-5 (2013).

Acknowledgements

RRA was partially supported by the Lancer Endowed Chair in Dermatology.

Author contributions

Conceptualization: BDL, YW, JT, RRA. Formal analysis: BDL. Funding acquisition: RRA. Investigation: BDL, YW. Methodology: BDL, YW. Supervision: JT, RRA. Writing—original draft: BDL. Writing—review & editing: YW, JT, RRA.

Competing interests
The authors declare no competing interests.

Additional information
Supplementary Information The online version contains supplementary material available at https://doi.org/10.1038/s41598-024-66235-2.

Correspondence and requests for materials should be addressed to B.D.L.

Reprints and permissions information is available at www.nature.com/reprints.

Publisher's note Springer Nature remains neutral with regard to jurisdictional claims in published maps and institutional affiliations.